Detection of Machine Lead in Ground Sealing Surfaces

F. Puente León[1], N. Rau[2]
[1]Lehrstuhl für Messsystem- und Sensortechnik, Technische Universität München, 80290 München
[2]DaimlerChrysler AG, Werk Untertürkheim, EP/MPL, 70546 Stuttgart
Submitted by G. Spur (1), Berlin, Germany

Abstract
During the finishing of contact surfaces of rotary shaft lip type seals, unwanted lead patterns may appear. Depending on the direction of rotation, these spiral marks may lead to early leakage or dry run, which may affect directly the longevity of the parts. New methods for satisfying the high requirements of the automotive industry are presented to determine the lead angle, the period length, and the number of starts. In contrast to earlier approaches, with a new fusion strategy, a robust extraction of the parameters of interest is attained even in the case of slightly pronounced lead structures. Moreover, by enhancing the measurement set-up with additional optical components, an in-line inspection becomes possible.

Keywords: Machine lead, Surface texture, Automated visual inspection

1 INTRODUCTION

The microscopic texture of ground sealing shaft surfaces consists of a superposition of straight, periodic lead grooves and short, stochastically placed grinding marks, as schematically shown in Fig. 1(left). The lead grooves show a helical course and generate an undesired pump behaviour. Depending on their direction of rotation, this may lead to leakage or dry run. To characterize the lead structures comprehensively, suitable data G of the surface have to be measured to extract quantitative estimates of the lead angle β, which typically adopts values in the range of a few minutes, as well as the period length d, the number of starts z, and the distinctness of the lead structures; see Fig. 1(left).

2 PREVIOUS WORK

An early approach to detect lead phenomena developed by the Freudenberg company is based on the analysis of the lateral displacement of a loaded thread while rotating the shaft to be examined [1]. Some disadvantages of this approach are the influence of the thread as well as an ambiguous detection threshold. Nevertheless, this fast testing method has established itself in practice due to its simplicity and its low costs.

Later on, the Mercedes-Benz company developed the CARMEN (*Computer Aided Roughness Measurement and Evaluation*) system to quantify machine lead. It performs an analysis of numerous 1-D signals measured with a mechanical stylus gauge and estimates the pertinent surface parameters using correlation methods [2].

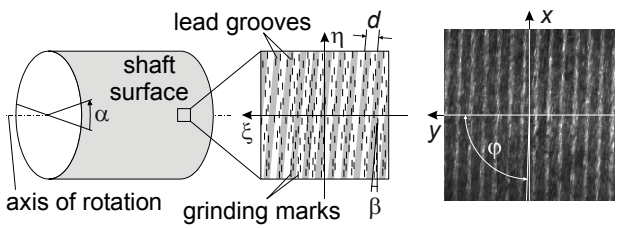

Figure 1: (left) Schematic representation of lead grooves (periodic) and grinding marks (stochastic) on a shaft; (right) grey level image $g(\mathbf{x})$ acquired with a microscope.

However, still today, long data acquisition times make a broad use of stylus instruments in production lines and measurement labs difficult [3].

Another approach to analyze machine lead is based on the application of scattered light methods [4]. However, the information obtained this way only enables one to determine the distinctness of the lead structures. The lead angle, which is very important in practice, cannot be estimated with sufficient precision with this strategy.

In contrast to the approaches discussed in this section, alternative optical as well as visual inspection methods enable the possibility of analyzing lateral geometric data in a fast and cost-efficient manner [5, 6]. Therefore, such approaches are especially suitable for an in-line assessment of sealing surfaces during production. Since visual inspection methods only register depth data indirectly, early tests have shown problems with regards to robustness, especially in the case of slightly pronounced lead structures [7, 8]. However, it can be shown that by means of a suitable illumination, meaningful information on topographical features, such as the distinctness of grooves, can be extracted reliably [8]. Unfortunately, the lack of a robust and sufficiently precise strategy to estimate the lead angle β and the period length d complicated the assessment of lead phenomena up till now.

3 MEASUREMENT PRINCIPLE

In Fig. 1(right), a grey level image $g(\mathbf{x})$ of a ground sealing surface acquired with a microscope is presented, where $\mathbf{x} = (x, y)^{\mathrm{T}} \in \mathrm{R}^2$ denotes the image coordinates. Whenever it is expedient, $g(\mathbf{x})$ will be considered as a continuous signal of infinite extent. However, to implement the presented methods on a computer, the consequences of spatial sampling and of restriction to a finite spatial extent have to be taken into account [9].

To image the lead marks with high contrast, a halogen lamp with a low angle of incidence is used as an illumination source [10]. The sensor employed is a CCD camera with $M \times N = 512 \times 512$ pixels.

In the following, the image $g(\mathbf{x})$ will be thought of as a realisation of a stochastic process. The spectral characteristics of the process can be described on the average

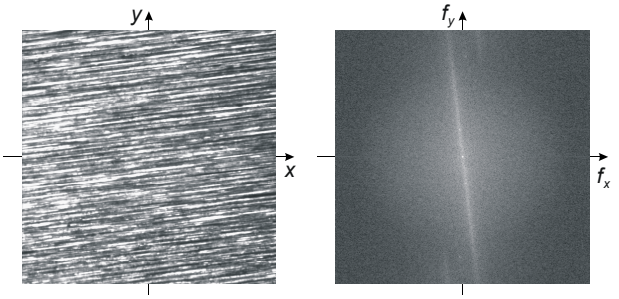

Figure 2: (left) Grey level image $g(\mathbf{x})$; (right) logarithm of the periodogram $\hat{S}_{gg}(\mathbf{f})$ of $g(\mathbf{x})$.

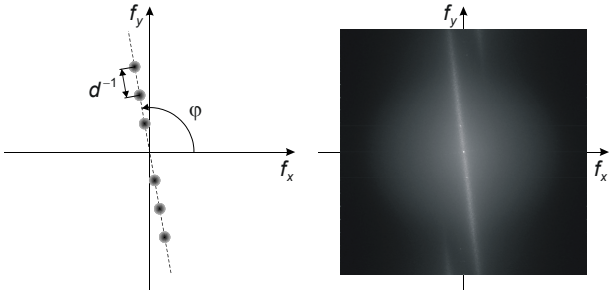

Figure 3: (left) Comb filter $K(\mathbf{f}; d, \varphi)$; (right) logarithm of the averaged periodogram $\overline{S}_{gg}(\mathbf{f})$.

by means of the power spectral density (PSD) function $S_{gg}(\mathbf{f})$ [11, 12]. In practice, the PSD function can be estimated by means of the so-called periodogram (PG)

$$\hat{S}_{gg}(\mathbf{f}) := \frac{1}{NM}\left|G(\mathbf{f})\right|^2 \quad \text{with} \quad G(\mathbf{f}) := \mathrm{F}\ \{g(\mathbf{x})\}\,, \tag{1}$$

where M and N describe the dimension of the image, and $\mathbf{f} = (f_x, f_y)^{\mathrm{T}} \in \mathrm{R}^2$ the spatial frequency [12]. If a texture shows straight, parallel grooves, the corresponding components of the PSD function concentrate along a straight line across the origin of the spatial frequency domain perpendicular to the band of grooves, as shown in Fig. 2 [11]. Moreover, if the grooves are periodic, such as in the case of lead marks, the PSD function adopts the shape of an equidistant comb of δ impulses [11].

A proven method to determine the groove angle φ is based on integrating the PG along radial lines [11]. The location of the global maximum represents an estimate $\hat{\varphi}$ of the dominant orientation of the band of grooves. Admittedly, the PG is an extremely unsuitable estimate of the PSD function, because it is not consistent, and its standard deviation is on the order of magnitude of the quantity to be estimated itself [12]. However, the fluctuations inherent to the PG can efficiently be reduced by means of the radial integration. This way, a very robust procedure to determine the groove angle is obtained.

If the measurement set-up is calibrated such that the angle of rotation γ between the image coordinates (x, y) and the lateral world coordinates (η, ξ) is known, the lead angle β can be extracted from the groove angle [8]:

$$\varphi := \beta + \gamma + 90°\,. \tag{2}$$

In case of small lead angles β, the determination of γ as well as the poor angular resolution of the radial integration may cause problems when applying this strategy.

In previous research [7, 8] it was proposed that the distance Δ^{-1} between the δ impulses of the PG be used to determine the period length d. For this purpose, a comb filter $K(\mathbf{f}; d, \varphi)$ according to Fig. 3(left) is dimensioned such that the power components corresponding to the lead marks coincide with the apertures of the filter. All in all, the determination of φ and d is performed by means of an optimization calculus according to the following equation:

$$(\hat{d}, \hat{\varphi}) := \underset{d,\varphi}{\operatorname{argmax}} \left\{ \iint K(\mathbf{f}; d, \varphi) \cdot \hat{S}_{gg}(\mathbf{f})\, \mathrm{d}\mathbf{f} \right\}. \tag{3}$$

This approach yields good results in the case of pronounced grooves; in the case of faint lead structures, however, the spectral components corresponding to the periodic grooves (i.e. the δ impulses) are very difficult to detect in the PG due to their small support region. In such cases, large variance of the PG leads regularly to errors [8]. To compensate these problems, a method is proposed in [8] that consists in calculating d from several images individually and then determining the average of the computed values. However, this procedure still leads to poor results. In contrast to the method of the radial integration of the PG, the estimation of the groove angle φ according to Eq. (3) does not completely exploit the information contained in the PG, especially in case of fluctuating groove amplitudes, which cannot be avoided due to illumination effects, among other things [10, 11].

A significantly more robust approach to estimate the parameters φ and d is based on the suppression of the fluctuations inherent to the PG by means of suitable image fusion methods. This step implies recording a series G of B images by systematically varying the angle of rotation α of the workpiece:

$$\mathrm{G} := \{g(\mathbf{x}, \alpha_i),\ i = 0, \ldots, B-1\}\,. \tag{4}$$

Since the information of interest regarding the PSD function is distributed over all realizations of the stochastic process, a concurrent fusion strategy is applied: by averaging the periodograms of the images $g(\mathbf{x}, \alpha_i)$, an enhanced estimate of the PSD function is obtained:

$$\overline{S}_{gg}(\mathbf{f}) := \frac{1}{BNM}\sum_{i=0}^{B-1}\left|G(\mathbf{f}, \alpha_i)\right|^2. \tag{5}$$

If uncorrelated periodograms are assumed, the variance of $\overline{S}_{gg}(\mathbf{f})$ is B times lower than the variance of $\hat{S}_{gg}(\mathbf{f})$ [12]. Compared with the increased measurement effort, a more robust parameter estimation is achieved without the need of sacrificing precision due to a lower spectral resolution, as would be the case if Bartlett's procedure of averaging periodograms was used [12].

4 SIGNAL PROCESSING

The signal processing algorithms described in the following subsections assume that an image series G of the object to be inspected has been recorded according to Eq. (4). The size B of the image series should be typically three to four times the maximum expected number of starts. The complete series will cover an angle of 360°:

$$\alpha_i = \alpha_0 + i\Delta\alpha\,, \quad i = 0, \ldots, B-1\,, \quad \Delta\alpha \cdot B = 360°\,. \tag{6}$$

The acquisition of the image series can be automated by using a suitable rotational positioning device [2].

4.1 Groove angle

To determine the groove angle φ, each image of the series $g(\mathbf{x}, \alpha_i)$ is windowed first with a Gaussian to reduce DFT leakage [13]. Following, the corresponding periodo-

grams $\hat{S}_{gg}(\mathbf{f},\alpha_i)$ are calculated according to Eq. (1) and then integrated along radial paths:

$$\varpi(\phi,\alpha_i) := \int_{f_y=0}^{\infty}\int_{f_x=-\infty}^{\infty}\hat{S}_{gg}(\mathbf{f},\alpha_i)\cdot\delta(\mathbf{f}^{\mathrm{T}}\mathbf{e}_{\phi\perp})\mathrm{d}\mathbf{f}\,, \tag{7}$$

$$\mathbf{e}_{\phi\perp} = (-\sin\phi,\cos\phi)^{\mathrm{T}}\,, \quad \phi\in[0°;180°)\,.$$

To compute Eq. (7), the values of the periodograms have to be interpolated on a polar lattice taking into account the sampling theorem of computer tomography [14]. Due to the symmetry of the PG, it is sufficient to calculate the integral $\varpi(\phi,\alpha_i)$ for the values $\phi\in[0°;180°)$.

For each image, the location of the global maximum of the integral $\varpi(\phi,\alpha_i)$ represents an estimate of the groove angle of the corresponding image $g(\mathbf{x},\alpha_i)$:

$$\varphi_i = \underset{\phi}{\mathrm{argmax}}\{\varpi(\phi,\alpha_i)\}\,. \tag{8}$$

Since the groove angle φ is invariant to the rotational position of the workpiece α, a dithering effect can be exploited to increase the angular resolution of this estimate. Thus, thanks to an additive noise component in the integrals $\varpi(\phi,\alpha_i)$, an improved estimate for the groove angle can be computed by averaging the angles φ_i obtained for the single images:

$$\hat{\varphi} = \frac{1}{B}\sum_{i=0}^{B-1}\varphi_i\,. \tag{9}$$

In contrast to Eq. (8), in this case the accuracy of $\hat{\varphi}$ is not limited by the discretization of the radial integration.

4.2 Period length

To enable a robust measurement of the period length d, an averaging of the periodograms $\hat{S}_{gg}(\mathbf{f},\alpha_i)$ is performed according to Eq. (5). Since with Eq. (9) a reliable estimate $\hat{\varphi}$ of the groove angle is available, the optimization scheme proposed in Eq. (3) can be simplified, and now a 1-D search is sufficient:

$$\hat{d} := \underset{d}{\mathrm{argmax}}\left\{\iint K(\mathbf{f};d,\hat{\varphi})\cdot\overline{S}_{gg}(\mathbf{f})\mathrm{d}\mathbf{f}\right\}. \tag{10}$$

This method leads to a relative accuracy of approximately 1% in the measurement range of interest (4–171 pixels/period). If necessary, the measurement range may easily be extended by modifying the magnification of the microscope used.

4.3 Number of starts and lead angle

Since the lead angle typically adopts values in the range of a few minutes, an absolute measurement of this angle is very difficult due to adjustment inaccuracies. Even if the angle γ would be known, the computation of φ according to Section 4.1 would not lead to a sufficiently precise estimate of β [13].

A notably more sensible approach is based on enlarging the surface area observed by the image sensor by rotating the shaft around its own axis. If this is accomplished by recording a series of images as in Eq. (4), a fixed image location $\mathbf{x}_0$ describes a trajectory in η direction over the entire series; see Fig. 4(left). This makes it possible to determine the lead angle β independently of the angle γ. The knowledge of the lateral displacement of a groove perpendicular to its course over a sufficiently large angular range $\varphi_2-\varphi_1$ would allow an accurate measurement of β.

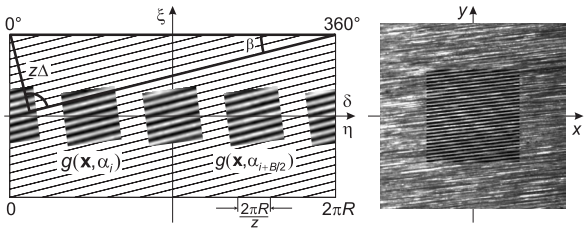

Figure 4: Determination of the number of starts and the lead angle: (left) schematic representation of the circumferential surface of a sealing shaft; (right) original image (edges) and result of the filtering (centre).

An alternative and computationally more efficient approach consists in analyzing the grey level intensities $g(\mathbf{x}_0,\alpha)$ of the images at the location $\mathbf{x}_0$ to determine the number of starts z first. However, in most cases the grinding grooves dominate over the lead marks, and it is thus not possible to count the starts by just evaluating the image intensities. To cope with this problem, the images can be filtered by means of a comb filter consisting of only those two central apertures that correspond with the fundamental oscillation of the lead marks; see Fig. 3(left). The resulting images only contain lead marks showing an almost ideal sinusoidal appearance; see Fig. 4(right).

The signal describing the intensities of the filtered images at the location $\mathbf{x}_0$ has a narrow bandpass characteristic. Consequently, if enough samples B are obtained in circumferential direction, it is possible to determine the number of starts z, e.g. by simply counting the zero crossings of this signal. Taking Fig. 4(left) into consideration, the following expression is obtained for the lead angle β:

$$\hat{\beta} = \arcsin(\hat{z}\hat{d}/2\pi R)\,, \tag{11}$$

where R denotes the radius of the workpiece. To detect the lead direction, i.e. the sign of the lead angle, a further surface point $\mathbf{x}_1$ at the distance $d/4$ to $\mathbf{x}_0$ perpendicular to the direction of the grooves has to be observed. Following, the phase delay of the corresponding signal with respect to the first signal has to be determined. In contrast to former approaches documented in [7, 8], this strategy does not require any adjustment of the visual inspection system.

5 RESULTS

To examine the presented methods, 9 thrust collars (R = 145 mm) showing different lead angles as well as differently pronounced lead marks have been measured. The same workpieces have also been analyzed with the computer-vision-based strategies described in [8], the results of which are referred to as “AS.” As a reference, the tactile system “CARMEN” has been chosen [2].

For each workpiece, B = 120 images of size $M\times N$ = 512×512 have been recorded according to Eq. (6). Subsequently, the images have been processed as described in Section 4.

Figure 5 shows the measurement results of the period length d for all three systems. Despite of the barely recognizable lead structures (see Fig. 4(right)), the presented method yields very robust results in all cases. In contrast, the system AS, which is based on a direct analysis of the periodogram according to Eq. (3), leads to significant errors in case of slightly pronounced lead grooves (workpieces nos. 2 and 27).

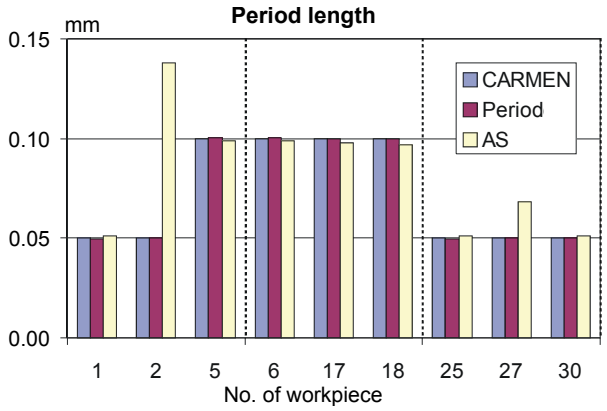

Figure 5: Comparison of the results for the period *d*.

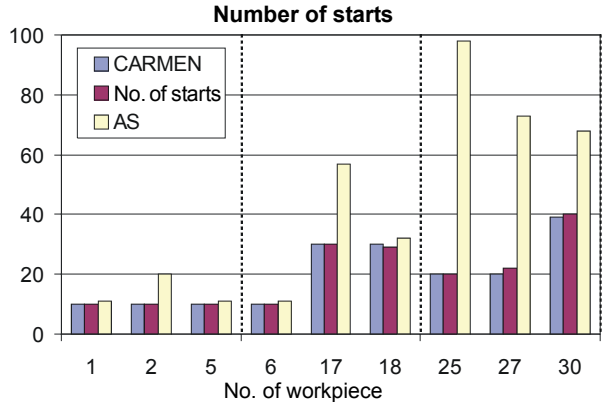

Figure 6: Comparison of the results for the no. of starts *z*.

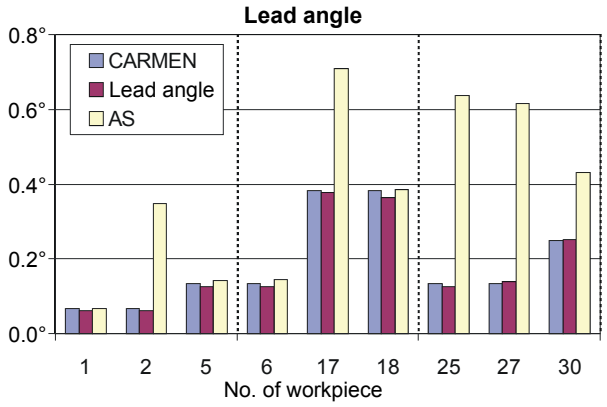

Figure 7: Comparison of the results for the lead angle β.

Also with the number of starts *z*, the results obtained closely correspond with the values computed by CARMEN. Only in 3 cases slight differences can be observed. However, these deviations are assumed to be due to rounding errors of the CARMEN system. To reduce the measurement effort, this system only records a relatively small angular section of the workpiece and extrapolates the result to 360 degrees.

Since the lead angle β is derived from the magnitudes *d* and *z*, see Eq. (11), it is not surprising that a reliable estimate can only be obtained if good measurements are available for *d* and *z*; see Fig. 7. Despite of the relatively large number of images to be processed, most operations can efficiently be performed by means of fast algorithms [8]. Thus, the analysis of the measured data only takes approximately one minute on a typical PC. The acquisition of the image series takes two minutes with the current experimental set-up.

6 OUTLOOK

After having demonstrated the suitability and the accuracy of the presented algorithms to measure lead structures, optimization strategies shall be discussed. In most cases, the distinctness of lead structures already allows a robust extraction of the period length *d* based on one or a few images [8]. Moreover, a measure introduced in [7] would enable a quantitative assessment of the reliability of this estimate. Especially in such cases, a more efficient strategy to determine the number of starts *z* would be desirable. If the filtering according to Subsection 4.3 could be performed by using analog optical components, the analysis of the signals of only two light sensitive sensors would suffice to determine *z*.

To suppress spectral components that do not correspond with the direction of the lead grooves, an adjusted cylindrical lens can be used. High frequency components complicating the counting of the periods can easily be suppressed by means of an out-of-focus optical mapping. After having determined *d* and adjusted the cylindrical lens automatically, further analysis of the sensor signals could take place in a few seconds. This would enable one to apply the proposed methods even to an in-line inspection of ground sealing surfaces.

7 ACKNOWLEDGMENTS

The authors would like to thank Mr. Frank Böhringer and Mr. Joshua Cohen for valuable comments on this paper.

[1] ESC Report, 2002, Wear sleeves & other shaft repair options, BSA, Glen Ellyn.

[2] Rau, N., Seibold, M., 1997, Drallstrukturen geschliffener Dichtflächen beurteilen, Werkstatt und Betrieb, 11.

[3] Lonardo, P.M., Lucca, D.A., De Chiffre, L., 2002, Emerging trends in surface metrology, CIRP Annals, 51/2.

[4] Baumgart, J., Rau, N., Truckenbrodt, H., 2000, Measurement of small, periodic undulations in surfaces, International Patent, WO 00/22377.

[5] Goch, G., 2003, Gear metrology, CIRP Annals, 52/2.

[6] Pfeifer, T., Wiegers, L., 1998, Adaptive control for the optimized adjustment of imaging parameters for surface inspection using machine vision, CIRP Annals, 47/1:487-490.

[7] Krahe, D., Beyerer, J., 1998, Quantifizierung von Drallerscheinungen an geschliffenen Wellendichtflächen mit Methoden der Bildverarbeitung. In: Sensoren und Meßtechnik, ITG-FB 148, VDE Verlag, Berlin, pp. 639-645.

[8] Krahe, D., 2000, Zerstörungsfreie Prüfung der Textur gehonter und geschliffener Gegenlaufflächen, VDI Verlag, Düsseldorf.

[9] Brigham, E.O., 1988, The fast Fourier transform and its applications, Prentice Hall, Englewood Cliffs.

[10] Puente León, F., 1997, Enhanced imaging by fusion of illumination series. In: Sensors, Sensor Systems, and Sensor Data Processing, Proc. SPIE 3100.

[11] Beyerer, J., 1995, Model-based analysis of groove textures with applications to automated inspection of machined surfaces, Measurement 15, 189-199.

[12] Oppenheim, A.V., Schafer, R.W., 1975, Digital Signal Processing, Prentice-Hall, Englewood Cliffs.

[13] Puente León, F., 1999, Automatische Identifikation von Schußwaffen, VDI Verlag, Düsseldorf.

[14] Bamler, R., 1989, Mehrdimensionale lineare Systeme, Springer-Verlag, Berlin.